RESPONSE TO THE REVIEWER 2.

We strongly appreciate the helpful comments of the reviewer with valuable suggestions and useful remarks, patently improving this work.

Next, we will try to answer and explain, in any case, all the questions. In addition, a new Figure and two more Tables have been added in the manuscript as a consequence of responding the reviewer's comments. Then, the Figures and Tables have been renumbered (starting from Figure 4 and Table 3). As a result the text has been accordingly modified to contain these changes, including new required calculations and results. In general, a revised manuscript containing all the necessary modifications is also available.

General:
The paper reports a long-range transport of Saharan dust. A dense set of optical observations with sun photometers and lidars, and in situ observations of the size distribution are presented. The material is original and appropriate for publication.

Details:

Page 6: The lidars suffer from overlap effects (laser beam with the field of view of the receiver). How large is this effect (height range before overlap is one), how is it corrected? How large are the uncertainties for the different systems?

We believe that details of overlap effects and their data correction procedures (uncertainties included) are out the scope of this work, since these questions have been addressed in previous works (Campbell et al., 2002; Wandinger and Ansmann, 2002; Welton and Campbell, 2002; Córdoba-Jabonero et al., 2008, 2009; Navas-Guzmán et al., 2011). However, we will try to clarify to some extent the reviewer's comments on this matter. Hence, a few modifications (see below) have been introduced in the manuscript (Section 3).

In Sect. 3.1.1:
"The MPL backscattered signal is registered in 1-minute integrated time and with a vertical resolution of 75 m, as for MPLNET requirements. MPL raw signal is corrected by several factors affecting the instrument, as described by Campbell et al. (2002), including the overlap correction. A detailed study on the uncertainties introduced in the raw signal correction from each of the instrumental effects for this kind of micropulse lidars can be found in Welton and Campbell (2002), being the overlap uncertainty the most dominant in the near-range. Finally, full-corrected profiles are hourly averaged in order to increase the signal-to-noise ratio (SNR).

In particular, a full overlap is reached at 5 km height for both MPLs. Corrections procedures reported in Campbel et al., (2002) have been performed in order to minimize uncertainties (Welton and Campbell, 2002). Above 500 m height a.g.l. overlap uncertainties are in the range of 10-50%, leading to errors of 10-40% in the data. Below 500 m height a.g.l. data are disregarded for the analysis due to too large errors by the intrinsic limitation of the system configuration."

In Sect. 3.1.2:
"Lidar backscattered signals are registered with 1-minute integrated time and a vertical resolution of 7.5 m. Full overlap is reached at around 1900 m a.s.l. (GRA station is located at 680 m a.s.l.). An overlap correction is then applied on the basis of the simple technique proposed by Wandinger and Ansmann (2002), down to the height where the overlap function is equal to 0.6-0.7. This correction allows

extending the profile in most cases down to 1200 m a.s.l., i.e. down to 500 m above the GRA station (Navas-Guzmán et al., 2011)."

In Sect. 3.1.3:
"AERONET Aerosol Optical Depth (AOD) is used to constraint the algorithm convergence by 'tuning' the lidar ratio (LR, extinction-to-backscatter ratio) values. Once the AOD convergence is obtained (less than 10%), a height-constant LR is estimated (errors of 15% are found from AOD convergence uncertainty). Thus, the 'guessed' extinction coefficients can be retrieved, and a lidar-derived hourly-integrated AOD is calculated from day- and night-time measurements. As stated before, due to the large overlap uncertainties below 500 m height a.g.l., data in this range are disregarded for that approach and then a BL homogeneously mixed is assumed instead."

The following references have been included, if not, in the references list:

Campbell, J.R., Hlavka, D.L., Welton, E.J., Flynn, C.J., Turner, D.D., Spinhirne, J.D., Stanley Scott III, V., and Hwang, I.H.: Full-time, eye-safe cloud and aerosol Lidar observation at atmospheric radiation measurement program sites: Instruments and data processing, J. Atm. Ocean. Tech., 19, 431-442, 2002.

Córdoba-Jabonero, C., Gil, M., Yela, M., Maturilli, M., and Neuber, R.: Lidar observations of Arctic aerosols and PSC detection in winter 2007 at the Koldewey station (Ny-Alesund, Norway). In: The second AWIPEV scientific workshop: French – German Polar Science on Spitsbergen during IPY, Bremen (Germany), 8 - 10 October, 2008.

Córdoba-Jabonero, C., Gil, M., Yela, M., Maturilli, M., and Neuber, R.: Polar Stratospheric Cloud observations in the 2006/07 Arctic winter by using an improved Micro Pulse Lidar. J. Atmos. Ocean. Techn., 26, 2136-2148, 2009.

Navas-Guzmán, F., Guerrero-Rascado, J.L., and Alados-Arboledas, L.: Retrieval of the lidar overlap function using Raman signals. Óptica Pura y Aplicada, in press, 2011.

Wandinger, U., and Ansmann, A.: Experimental determination of the lidar overlap profile with Raman lidar. Appl. Opt., 41, 511-514, 2002.

Welton, E.J., and Campbell, J.R.: Micropulse Lidar Signals: Uncertainty Analysis. J. Atm. Ocean. Tech., 19, 2089-2094, 2002.

Page 11, section 5.2.1 a: Please discuss the impact of overlap correction uncertainties.

In the frame of SPALINET, a complete study on lidar system and data retrieval intercomparison (Sicard et al., 2009) was carried out. Results from that work reflect indirectly the impact of the instrument corrections on lidar signal uncertainties, and they can be extrapolated the same way to the current measurements of this work (in particular, Sect. 5.2). Indeed, both SCO and GRA lidars were involved in that study. Full-corrected data (overlap correction included) and then retrieved backscatter coefficients profiles were found to be inside the uncertainty values allowed as for the EARLINET quality control tolerances (Matthias et al., 2004) followed in that intercomparison, i.e., the mean and standard deviations for the backscatter at 532 nm between lidar systems stayed below the maximum allowed values fixed (20% and 25%, respectively). ARN system was tested against the Koldewey Aerosol Raman Lidar (KARL), managed by the Alfred-

Wegener Institute (AWI, Germany) and devoted to long-term Arctic aerosol observations. In particular, both lidars were vertically pointing under free-aerosol conditions for overlap approach in the near-range. Once overlap was estimated, full-corrected data and their uncertainties were obtained. Backscatter coefficients profiles were retrieved and compared to the KARL measurements in the near-range for polar tropospheric aerosols and in the far-range for PSC detection. Intercomparison results showed a good agreement on instrument performance and data retrieval between both datasets (Córdoba-Jabonero et al., 2008, 2009; personal communication of R. Neuber and C. Córdoba-Jabonero).

This statement has been included in the end of Section 3.1.3.

The following references have been included, if not, in the references list:

Córdoba-Jabonero, C., Gil, M., Yela, M., Maturilli, M., and Neuber, R.: Lidar observations of Arctic aerosols and PSC detection in winter 2007 at the Koldewey station (Ny-Alesund, Norway). In: The second AWIPEV scientific workshop: French – German Polar Science on Spitsbergen during IPY, Bremen (Germany), 8-10 October, 2008.

Córdoba-Jabonero, C., Gil, M., Yela, M., Maturilli, M., and Neuber, R.: Polar Stratospheric Cloud observations in the 2006/07 Arctic winter by using an improved Micro Pulse Lidar. J. Atmos. Ocean. Techn., 26, 2136-2148, 2009.

Matthias, V., Bösenberg, J., Freudenthaler, V., Amodeo, A., Balis, D., Chaikovsky, A., Chourdakis, G., Comerón, A., Delaval, A., De Tomasi, F., Eximann, R., Hågård, A., Komguem, L., Kreipl, S., Matthey, R., Mattis, I., Rizi, V., Rodríguez, J.A., Simeonov, V., and Wang, X.: Aerosol lidar intercomparison in the framework of the EARLINET project-Part 1: Instruments. Appl. Opt., 43, 4, 961–976, 2004.

Sicard, M., Rocadenbosch, F., Reba, M.N.M., Comerón, A., Tomás, S., García-Vízcaino, D., Batet, O., Barrios, R., Kumar, D., and Baldasano, J.M.: Seasonal variability of aerosol optical properties observed by means of a Raman lidar at an EARLINET site over Northeastern Spain. Atmos. Chem. Phys., 11, 175–190, 2011.

Page 12, section 5.2.2: Again, how large is the error in the lidar ratio retrieval because of uncertainties in the overlap correction. Is certainly of the order of 20-50%.

Additional calculations have been made, obtaining errors in LR retrievals of 25-50% because of overlap correction uncertainties (10-50%).

Why are lidar ratios obtained with Raman lidar not shown, they are not affected by overlap effects. Should be improved.

Unfortunately, despite the GRA system is a Raman lidar (unlike the MPL-3 and MPL-4 systems) no Raman measurements were performed on 14 March 2008 (1-day dusty episode over GRA site). There was no coincidence with the EARLINET standard Raman measurement protocol (Mondays and Thursdays around sunset), and only GRA particular observations were performed at only day-time hours during the dust event monitored in this study.

Page 15: I checked the AERONET website. There are a plenty of trustworthy size distributions retrieved for ARN and GRA on 14 and 15 March 2008 (level 1.5).

Level1.5 is sufficient (level 1.5 should be stated). The level 1.5 data should than be plotted together with the in situ size distributions (in Figure 11) and the differences should be discussed. How do the effective radii match, is one of the interesting questions, as mentioned by Muller 2010? This would be a highlight of the paper. It is not acceptable that AERONET level 1.5 data are just ignored, although they clearly indicate the dust mode of the size distribution.

According to the reviewer's suggestions, the AERONET columnar-integrated volume size distributions ($VSD^{AERONET}$) together with a comparative analysis with the in-situ data in terms of the ratio of the fine-to-total mode ($V_{F/T}^{AERONET}$) of the $VSD^{AERONET}$ and the effective radius ($r_{eff}^{AERONET}$) have been included. In consequence, and due to the text structure followed in this article (the columnar-integrated observations appear before the in-situ data), a new Figure 4 and the Table 3 have been added in Section 5.1.1 and the Table 6 in Section 5.3.2. All other subsequent figures and tables have been renumbered afterwards. The comparison between columnar-integrated and ground-level volume size distributions has been presented at the end of Section 5.3.2. In addition, Figure 11 (renumbered as Figure 12) has also been modified to get a coincidence in time between the columnar-integrated and ground-level volume size distributions. The modifications are:

1) The following text has been included at the end of the Section 5.1.1:

"The impact of the mineral dust over the South of the Iberian Peninsula on 14 March is also observed from AERONET columnar-integrated size distributions ($VSD^{AERONET}$). The available $VSD^{AERONET}$ for the dusty (14 March) and non-dusty (15 March) days in ARN and GRA sites are shown in Fig. 4a and 4b, respectively, and the ratio of the fine-to-total mode of the $VSD^{AERONET}$ ($V_{F/T}^{AERONET}$) and the effective radius ($r_{eff}^{AERONET}$) for the total, fine and coarse modes of those $VSD^{AERONET}$ are shown in Table 3. A $V_{F/T}^{AERONET}$ value of 0.08 is found for the dusty case in both stations, highlighting a predominance of coarse mode particles over the total distribution (see Fig. 4). In addition, the typical downward trend of the $r_{eff}^{AERONET}$ for the coarse mode during dusty episodes (Noh et al., 2008; Prats et al., 2008) is also observed in both sites, being more significant in the GRA case."

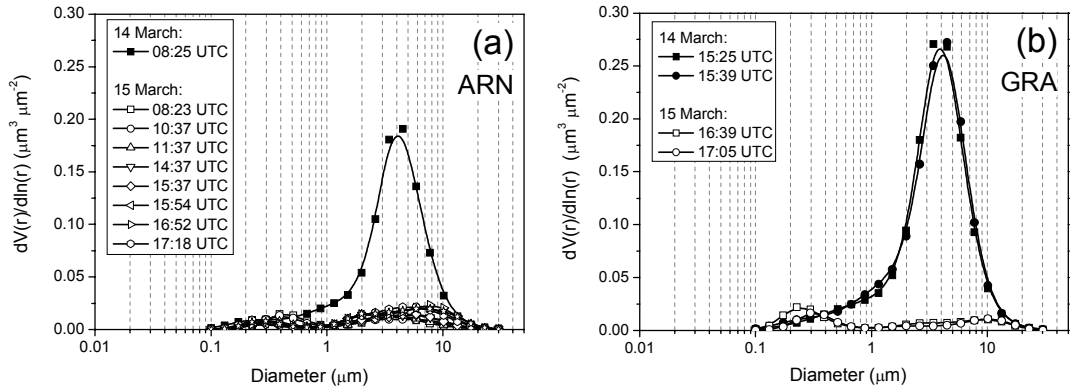

Figure 4. AERONET columnar-integrated volume size distributions ($VSD^{AERONET}$) at available times on 14 March (dusty day, full symbols) and 15 March (non-dusty day, open symbols) in ARN (a) and GRA (b) sites.

Table 3. AERONET fine-to-total mode ratio ($V_{F/T}^{AERONET}$) and effective radius ($r_{eff}^{AERONET}$) (in μm) for the total (T), fine (f) and coarse (c) modes (SD denotes standard deviation).

	'El Arenosillo' (ARN)				Granada (GRA)			
	$V_{F/T}^{AERONET}$	r_{eff}^{T} (SD)	r_{eff}^{f} (SD)	r_{eff}^{c} (SD)	$V_{F/T}^{AERONET}$	r_{eff}^{T} (SD)	r_{eff}^{f} (SD)	r_{eff}^{c} (SD)
Dusty	0.08 (*)	0.94 (*)	0.16 (*)	1.69 (*)	0.08 (0.01)	1.01 (0.05)	0.19 (0.01)	1.62 (0.01)
Non-dusty	0.24 (0.12)	0.54 (0.11)	0.15 (0.02)	1.72 (0.09)	0.49 (0.05)	0.27 (0.06)	0.14 (0.02)	1.99 (0.06)

(*) Just one value is available.

2) The particle volume size distributions and the ratio of the fine-to-total mode at ground level, which are analyzed in Section 5.3.2, are now denoted as VSD^{GL} and $V_{F/T}^{GL}$ respectively, in order to differentiate them from the columnar-integrated quantities gathered from AERONET analyses ($VSD^{AERONET}$ and $V_{F/T}^{AERONET}$).

3) The text in Section 5.3.2 "$V_{F/T}$ values of around 0.1 correspond to the presence ... regular values below 0.5 were reported", has been modified as follows:

"$V_{F/T}^{AERONET}$ values of around 0.1, similar to those obtained for the $VSD^{AERONET}$ on 14 March at 08:25 UTC (see Fig. 4 and Table 3), correspond to the presence of dust particles as based on previous results on columnar-integrated aerosol characterization in ARN site (Prats et al., 2008)."

4) The following text has been included at the end of the Section 5.3.2 a, i.e., after the paragraph (in Sect. 5.3.2 a) ending as "…only 250 km away.":

"$VSD^{AERONET}$ data associated to the dust occurrence on 14 March, as previously presented in Sect 5.1.1, are only available at 08:25 UTC in ARN (see Fig. 4a) and at 15:25 UTC and 15:39 UTC in GRA site (see Fig. 4b). At these times, in-situ measurements indicate that the dust intrusion was just starting to be observed at ground-level. This fact evidences clearly the differences found between columnar-integrated measurements and the ground-level boundary layer data as a result of the time required for the gravitational settling of the lofted aerosol particles associated to the arrival of Saharan dust over the study area.

In order to analyze the particle size more influential in relation to the aerosol in-situ optical parameters, the r_{eff}^{GL} has been calculated from the VSD^{GL} data. r_{eff}^{GL} is defined as the ratio of the third-to-second moments of the VSD^{GL}, and the values for the total concentration, the fine mode (size ranges: TV0 and TV1) and the coarse mode (size ranges: TV2 and TV3) are shown in Table 6. During the ARN dust event on the surface, r_{eff}^{GL} for the coarse mode decreases, ranging from 1.72 μm to 1.08 μm. However, this continuous decreasing behaviour is not detected in GRA site. Despite an initial r_{eff}^{GL} decrease for the coarse mode is observed from 14

March at 22:00 UTC to 15 March at 02:00 UTC, with values ranging from 1.29 μm to 1.14 μm, close to 07:00 UTC this trend is modified. This change can be explained because of the re-suspension of particulate matter from urban paved roads due to traffic early in the morning, obtaining higher r_{eff}^{GL} values for the coarse mode (Lyamani et al., 2008, 2010).

Both r_{eff}^{GL} and $r_{eff}^{AERONET}$ are analysed for comparison purposes. A strong dust occurrence as observed from the columnar-integrated data seems to have only a light influence on the surface when ground-level in-situ measurements are analysed (i.e., on 14 March at about 09:00 UTC and 16:00 UTC in ARN and GRA sites respectively, see Fig. 4). Hence, AERONET inversion data are about a factor of 5.5 and 1.6 higher than in-situ measurements for the total and fine mode, respectively, of the VSD^{GL} in ARN site. This factor (the ratio $r_{eff}^{AERONET}/r_{eff}^{GL}$) is about 1.1 ± 0.1 for the VSD^{GL} coarse mode in both ARN and GRA sites. These $r_{eff}^{AERONET}$ values are higher (see Tables 3 and 6) because the concentrations for the TV1 (fine) and TV2 and TV3 (coarse) size ranges of the columnar-integrated $VSD^{AERONET}$ are higher than those found on the ground level. This ratio $r_{eff}^{AERONET}/r_{eff}^{GL}$ is also analysed for non-dusty conditions (see Fig. 4). $r_{eff}^{AERONET}/r_{eff}^{GL}$ values of 1.4 ± 0.3 and 1.2 ± 0.2 are found for the total concentration and fine mode fraction, respectively, in ARN site. This ratio is about 1.5 ± 0.1 for the coarse mode in both sites. In any case, AERONET retrievals still provide larger effective radius than those obtained from ground-level in-situ measurements. However, these results are contrary to those reported by Muller et al., (2010a), where AERONET and airborne in-situ measurements at 3247 m and 4853 m were compared under dusty conditions. In this work, the particle effective radius from the AERONET algorithm turned out to be smaller.

Hence, these differences respect to AERONET data are positive or negative, depending on the in-situ measurements platform, either airborne or ground-level, respectively. This apparent discrepancy on the incidence behaviour of the dusty episode, together with the analysis of closest-to-surface backtrajectories (see Section 5.3.1), reflect a clear dependence of the VSD and the r_{eff} for dust particles on height. Then, further vertical size-resolved observations are needed for assessment of the impact on surface of the Saharan dust arrival to the Iberian Peninsula. ”

Table 6. Effective radius (r_{eff}^{GL}) (in μm) for the total (T), fine (f) and coarse (c) modes in ARN site and for the coarse mode (c) in GRA site, as calculated from ground-level in-situ particle size distribution observations.

‘El Arenosillo’ (ARN)				Granada (GRA)	
Time (UTC)	r_{eff}^{T}	r_{eff}^{f}	r_{eff}^{c}	Time (UTC)	r_{eff}^{c}
14 March 2008					
09:00	0.17	0.10	1.52	00:00	1.06
15:00	0.3	0.10	1.72	15:00	1.50
15 March 2008					
02:00	0.36	0.12	1.14	02:00	1.14
05:00	0.19	0.12	1.08	07:00	1.29
12:00	0.35	0.15	1.12	16:00	1.38

5) The Figure 11 (renumbered as Figure 12) has been modified to show the ground-level volume size distributions (VSD^{GL}) most coincident in time with the AERONET ones ($VSD^{AERONET}$, see Fig. 4).

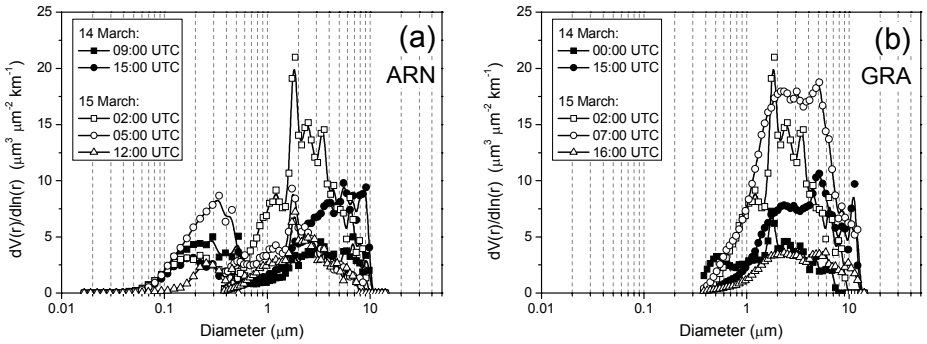

Figure 12. Ground-level volume size distributions (VSD^{GL}) from in-situ measurements at selected times on 14 March (dusty day, full symbols) and 15 March (non-dusty day, open symbols) in ARN (a) and GRA (b) sites.

6) The following text in Section 5.3.2: "Unfortunately, as stated before, comparison between both columnar-integrated … dusty episode over both ARN and GRA stations.", has been eliminated.

7) The following texts have been added in the Conclusions section to reflect the discussion of the new obtained results:

- After the paragraph ending as "… the second one is associated to a slower horizontal movement for the large particles.":

"Despite the scarce AERONET volume size distributions ($VSD^{AERONET}$) available during the dusty period in both ARN and GRA sites, the retrieved effective radius was compared with those calculated from the most coincident in time ground-level in-situ measurements. The ratio $r_{eff}^{AERONET}/r_{eff}^{GL}$ presents values higher than 1, in particular, 5.5 and 1.6 for the total concentration and the fine mode fraction of the VSD, respectively, as obtained in ARN site, and 1.1 for the coarse mode in both ARN and GRA sites. These results ($r_{eff}^{AERONET} > r_{eff}^{GL}$) as compared to those opposite obtained by Müller et al. (2010a), where AERONET and airborne in-situ measurements were performed, reveal a clear dependence of the dust particles properties on height, as reflected by the different in-situ measurements platform (either ground-level or airborne) used. Therefore, further vertical size-resolved observations are needed for a more complete understanding of the dust particles properties, and then for assessment of the impact on surface of the Saharan dust arrival to the Iberian Peninsula."

- After the paragraph ending as "… between microphysical and optical properties.":

"Moreover, height-resolved measurements are more and more required for aerosol research to understand the particular trends in the data as obtained from different technologies and measurements platforms. In particular, together with the methodology used in this work, the use of airborne aerosol instrumentation and the development of new lidar inversion algorithms can play a relevant role in this

understanding. In this sense, further aerosol research campaigns focused on aerosol microphysical properties retrieval are going on, involving both aerosol airborne and lidar instrumentations."

7) The following references have been included, if not, in the references list:

Lyamani, H., Olmo, F. J., and Alados-Arboledas, L.: Light scattering and absorption properties of aerosol particles in the urban environment of Granada, Spain, Atmos. Environ., 42, 2630–2642, 2008.

Lyamani, H., Olmo, F. J., and Alados-Arboledas, L.: Physical and optical properties of aerosols over an urban location in Spain: seasonal and diurnal variability. Atmos. Chem. Phys., 10, 239–254, 2010.

Müller, D., Weinzierl, B., Petzold, A., Kandler, K., Ansmann, A., Müller, T., Tesche, M., Freudenthaler, V., Esselborn, M., Heese, B., Althausen D., Schaladitz, A., Otto, S. And Knippertz. Mineral dust observed with AERONET Sun photometer, Raman lidar, and in situ instruments during SAMUM 2006: Shape-independent particle properties. J. Geophys. Res., 115, D07202, doi:10.1029/2009JD012520.

Noh, Y.M., Kim, Y.J., Müller, D.: Seasonal characteristic of lidar ratios measured with a Raman lidar at Gwangju, Korea in spring and autumn. Atmos. Environ., 42, 2208-2224, 2008.